Carbon Capture Science & Technology 13 (2024) 100231

Contents lists available at ScienceDirect

Carbon Capture Science & Technology

journal homepage: www.elsevier.com/locate/ccst

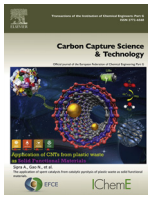

Full Length Article

Storage capacity estimates and site conditions of potential locations for offshore-wind powered carbon dioxide removal and carbon sequestration in ocean basalt

Heather Norton[a,*], Devin Todd[b], Curran Crawford[a]

[a] Institute for Integrated Energy Systems (IESVic), University of Victoria, PO Box 1700 STN CSC, Victoria, BC V8W 2Y2, Canada
[b] Pacific Institute for Climate Solutions (PICS), PO Box 1700 STN CSC, Victoria, BC V8W 2Y2, Canada

ARTICLE INFO

Keywords:
Carbon dioxide removal (CDR)
Offshore wind
Carbon capture and storage (CCS)
Negative emissions technology (NET)
Basalt

ABSTRACT

Negative emission technologies (NETs) are considered essential to keep global warming below 2 °C. Situating wind-powered carbon dioxide removal (CDR) devices offshore and injecting carbon dioxide (CO2) into deep-water sub-seafloor basalt aquifers has the potential to offer large CO2 removal capacity. It also avoids land and water-use competition and provides additional low-risk protections against post-injection leakage compared to terrestrial CO2 storage. This paper seeks to identify locations where offshore wind and potential basalt storage locations exist within close proximity to one another around the globe. A global mean wind power density map at 150 m height was computed using 30 years (1986–2016) of ERA5 hourly wind speed reanalysis data. Offshore regions with mean wind speed greater than 8 m/s were identified. Offshore regions with basalt aquifers along seismic or aseismic ridges which provide potential CO2 storage sites were identified and selected based on sediment thickness, age, and distance from plate boundaries. Four scenarios were constructed to capture a range of constraints with implications for technical, economic and regulatory difficulties. For each scenario, eligible regions for CO2 injection were filled by regularly spaced grid points and the distance to the nearest eligible wind resource was calculated for each point to identify the most promising configurations. Total available storage capacity within reach of wind resources was estimated to be between 4,300Gt and 196,000Gt depending on both uncertainties in porosity and other imposed constraints; even the most conservative estimates represent enormous capacity compared to global targets for negative emissions technologies. Typically, the best areas were found close to the poles due to the greater prevalence of good wind resources in those areas. Site-specific properties such as water depth and distance from shore are computed for the identified locations in order to characterize the conditions in which such locations are typically found.

1. Introduction

1.1. Coupling offshore-wind, direct air or ocean capture, and ocean basalt storage

As global emissions reductions fail to keep pace with emissions targets, Negative Emissions Technologies (NETs) are gaining increasing attention (Intergovernmental Panel on Climate Change, 2023). For example, the International Panel for Climate Change Sixth Assessment Report estimated that to limit warning to two degrees Celsius or below, 168–763 Gt of bio-energy carbon capture and storage (BECCS) and 0–339Gt CO2 of direct air capture with storage (DACCS) would be required, both of which require geological storage of CO2 (Pathak et al., 2022). While there are many proposed NETs, each with their own strengths and weaknesses (Rueda et al., 2021), direct air and ocean capture devices have received considerable attention. However, due to their substantial energy requirements, the carbon dioxide removal efficiency of many such devices is strongly influenced by the carbon intensity of their power source (Madhu et al., 2021). Therefore, in order for these devices to provide efficient carbon dioxide removal (CDR) on a climate-relevant scale, large quanties of clean power will be essential. Offshore wind has vast unused potential that could be used for this purpose. For example, Ishaq and Crawford showed that it was possible to meet direct air capture energy demands for 11 Gt/year of CO2 removal using between 5.3 and 5.6 % of the world's offshore wind technical potential (Ishaq and Crawford, 2022). In order for such a system to provide negative emissions, long term carbon dioxide storage is also required. This would ideally be located in proximity to the power source and capture devices in order to reduce transport costs. Injecting carbon dioxide into subsea basalt has been proposed as a means of permanent CO2 storage that benefits

* Corresponding author.
E-mail address: heathernorton@uvic.ca (H. Norton).

https://doi.org/10.1016/j.ccst.2024.100231
Received 26 February 2024; Received in revised form 9 May 2024; Accepted 18 May 2024

from multiple trapping mechanisms to support storage security: lower permeability sediment which provides stratigraphic trapping, geochemical trapping due to reaction with basalt, and properties of CO2 at depth which should help it to stay underwater (Goldberg et al., 2008). Potential storage capacity in basalt is more plentiful offshore than onshore (Oelkers et al., 2023). Goldberg and Slagle (2009) showed that vast storage potential existed in multiple offshore areas around the world. This paper therefore considers offshore wind-powered carbon dioxide removal coupled with ocean basalt storage. It draws inspiration from a concept for on-shore wind with direct air capture and ocean basalt storage which was proposed by Goldberg et al. (2023, 2013). Such a system would have multiple advantages. Direct air capture is not limited by land or feedstock availability in the same way as BECCS or reforestation approaches (Fuss et al., 2018). If using direct ocean capture (DOC) devices, the system would be naturally co-located with the required seawater feedstock. The system could be placed far enough offshore to use the vast renewable energy resources which are unlikely to be financially viable for land-based electrification and decarbonization efforts. The use of offshore wind turbines could provide a co-located low-carbon energy source to support efficient net CO2 removal by the system and obviate the transmission limitations of grid-connected offshore turbines. Offshore wind continues to enjoy cost reductions and is among the most globally scalable and deployable energy generation sources. It also eradicates concerns residents may have with installations nearby to their locations (so-called 'Not-In-My-Back-Yard' issues). Consequently, a CDR concept using wind-powered carbon dioxide removal coupled with ocean basalt storage would have many advantages that support rapid deployment to a climate-relevant scale.

1.2. Technological development to date

Offshore wind already boasts more than 50GW of installed capacity (Musial et al., 2022), but most installations are limited to water depths of 200 m or less (Edwards et al., 2023). Considerable development has already been undertaken for both DAC and offshore basalt storage technologies. Leading DAC technologies typically use solid sorbents or aqueous solvents to capture CO2 (Wilcox et al., 2021). For example, Climeworks built its first solid sorbent demonstration plant in 2011 and commissioned its first commercial DAC plant, which captured approximately 900 t/year of CO2, in 2017 (Gutknecht et al., 2018). Project Orca, capturing approximately 4kt/year of CO2 using solid sorbent technology and injecting it into onshore basalt, commenced operation in September 2021 (Climeworks, 2021). Keith et al. (2018) have designed and provided cost estimates for a 1 Mt/year liquid solvent based capture plant. They also reported on the performance of a pilot plant, and construction of a large-scale plant capturing approximately 0.5 Mt/year commenced in 2022 (Carbon Engineering, 2023). At the time of writing, the IEA currently tracks 13.6Mt/year direct air capture projects that are planned to commence operation by 2030 (IEA, 2023). However, offshore direct air capture is currently limited to academic study (Foxall et al., 2023a, 2023b; Ishaq and Crawford, 2022; Nawaz et al., 2023; Nawaz and Satterfield, 2024; Satterfield et al., 2023; Shehzad et al., 2023; Webster et al., 2024). Foxall et al. considered prospects for direct air capture onboard floating wind turbines (Foxall, 2023; Foxall et al., 2023a, 2023b). Although susceptible to performance reductions from airborne salt particles, they concluded that solid sorbent systems were more suitable for offshore implementation than liquid solvent systems. Multiple barriers to offshore implementation of liquid solvent systems were identified, including large unit sizes, sensitivity to dynamic motion, and transportation limitations on feedstock and waste products. In addition to direct air capture, there are multiple technologies under development for direct ocean capture (DOC), which capture carbon dioxide from seawater to release a pure stream of CO2 for downstream utilisation or storage (Digdaya et al., 2020; Eisaman et al., 2018; Hornbostel et al., 2022; Kim et al., 2023; Rivero et al., 2023); of these, Captura's technology is the most developed with plans for two pilot sites (Captura, 2023a, 2023b), both of which take place on the shoreline rather than offshore.

When it comes to storage, The Carbfix project (Clark et al., 2020; Matter et al., 2016, 2009; Pogge von Strandmann et al., 2019; Sigfússon et al., 2018) and the Wallula project (White et al., 2020) have both demonstrated CO_2 storage with mineralization in basalt onshore. The Mammoth project, under construction at the time of writing, combines direct-air-capture and injection into onshore basalt storage and has a target capacity of 36kt/year (Carbfix, 2022). There are existing offshore CO2 storage projects injecting into depleted gas fields (Chadwick and Eiken, 2013) and saline aquifers under the seabed (Tanaka et al., 2017), with multiple offshore carbon capture and storage projects currently at the planning stage (Luo et al., 2023). For example, Norway continues to progress this technology on a large scale; the first phase of the Longship project plans to be operational in 2024 with a storage capacity of 1.5 Mt/year (Northern Lights, 2023). Although no commercial projects currently inject into ocean basalt offshore, the Cascadia CarbonSAFE project completed a pre-feasibility study on storing 2.5 Mt/y (million tonnes per year) of carbon dioxide in an ocean basalt reservoir off the coast of Washington State and British Columba (Goldberg et al., 2018a). A range of scientific studies further support the use of offshore basalt for CO_2 storage (Awolayo et al., 2022; Ekpo Johnson et al., 2023; Goldberg et al., 2008; Nelson et al., 2022; Rosenqvist et al., 2023; Slagle and Goldberg, 2011; Tutolo et al., 2021).

1.3. Global mapping

Areas with potential for ocean basalt storage have been mapped in the past (Goldberg and Slagle, 2009; Marieni et al., 2013; Pilorgé et al., 2021; Planke et al., 2021; Snæbjörnsdóttir et al., 2020) and estimates of their capacities undertaken (Goldberg and Slagle, 2009; Marieni et al., 2013; Snæbjörnsdóttir et al., 2014). Pilorgé et al. (2021) mapped areas where wind power and global basalt rocks were directly co-located. However, they did not assess storage capacities, nor allow for wind resources that are located within proximity of injection sites. In addition, to the best of our knowledge, little is known about the site conditions at which subsea basalt locations are found. Particularly since younger basalt (which is likely to be porous and permeable) is often found close to plate boundaries far from shore, site conditions such as extreme water depths may pose a real barrier to project implementation. In all cases, site conditions have implications for the quantity and type of infrastructure that needs to be deployed to implement a CO2 storage project, which ultimately impacts economic competitiveness. Therefore, site conditions must be well characterized to situate projects most effectively and to inform engineering design efforts. This paper therefore identifies priority locations where an offshore wind powered carbon dioxide capture with ocean basalt storage system could be incrementally situated around the globe. We then assess potential storage capacities of such areas to determine if they are significant enough to make meaningful contributions towards NETs being able to operate at the Gt scale. First global areas which would be suitable for ocean basalt storage (Section 2.1) and offshore wind farms (Section 2.2) are mapped. Locations of major ports are also mapped (Section 2.3) to determine whether storage locations are closer to wind resources for powering capture or to ports which might be used for CO2 transport from point source capture locations onshore. Ports would also be required to support deployment and servicing of the offshore assets. Multiple scenarios are constructed, imposing constraints which imply differing levels of difficulty from a technological or regulatory standpoint (Section 2.4). The distances between suitable storage locations, wind resources, shorelines, and ports are then calculated (Section 2.5) and the total storage capacities associated with different sets of constraints are estimated (Section 2.5). This allows the sensitivity of global capacity estimates to differing constraints to be assessed (Section 3.1), and the most promising areas to be identified (Section 3.2). These results are then discussed in the context of financial and technological uncertainties (Sections 4.1–4.3).

2. Methods

This analysis seeks to identify locations with high-level potential for the proposed concept using an approach that is simple enough to be applied at a global scale and relevant to many different technological implementations. To determine the suitability for ocean basalt storage, constraints are imposed for basalt age and formation mechanism, sediment thickness, and distance from plate boundaries (Goldberg and Slagle, 2009). The constraints for offshore wind focused on wind energy potential, determined based on mean wind speed from global reanalysis data. This allows for wind potential to be assessed at a global level without being conditional on the power curve of a particular turbine. For constraints that have been proposed which may not be necessary, such as injecting in locations with very deep water to provide additional security through gravity trapping, separate scenarios were constructed with different combinations of optional constraints to provide a range of estimates. Since the maximum distance between wind resources and injection location that would be considered viable for project implementation depend on many different factors, no single limit was applied. Rather, the distance to the nearest wind resource was reported for all injection sites that met the imposed constraints for the given scenario to allow for a more nuanced discussion. Storage capacity for injection locations was estimated by considering the area of the injection location along with reasonable values for reservoir depth and porosity. The values used within the limits and capacity estimates (e.g. for basalt age and porosity, mean wind speed) are set conservatively where there is uncertainty around the most appropriate value to use. Nevertheless, it should be noted that some locations identified using this high-level approach would likely prove unsuitable for reasons that are outside the scope of the analysis (such as the presence of seismic activity or a marine protected area).

2.1. Storage

First the locations which are most likely to have ocean basalt suitable for storage were identified (Fig. 2a). Previous studies have shown that ocean ridges caused by seafloor spreading (seismic ridges) typically include permeable basalt covered by impermeable sediment such that storage is possible (Goldberg et al., 2008). Due to reactions between basalt and sea water which fill in the pores over time, ridges aged less than 10–15 million years are sought to preserve sufficient permeability for injection and storage (Goldberg et al., 2018b; Goldberg and Slagle, 2009). The age of ocean basalt was taken from a global deep-time plate motion model published by Müller et al. (2019). Using GIS, areas with seismic ridges were identified and restricted to areas with age less than 15 million years (see supplementary Fig. 1). Following previous global mapping exercises (Goldberg and Slagle, 2009; Snæbjörnsdóttir et al., 2020), deep sea basalt formed on the seafloor by intra-plate volcanism (otherwise known as aseismic regions or Large Igneous Provinces) are also included without an age restriction. This is based on their proposed suitability for storage due to the high permeability and porosity of the lava flow, and the presence of interbedded low-permeability layers which may act as seals until mineralization has occurred (McGrail et al., 2006). There is less available information from drilling in offshore flood basalts (Coffin et al., 2006), but modelling efforts informed by onshore regions have been used to infer the presence of promising aseismic offshore sequences for CO2 storage (Rosenqvist et al., 2023). Areas with large igneous provinces were identified using data from Coffin et al. (2006) (see supplementary Fig. 2).

However, ocean basalt areas may still be unsuitable for storage. Firstly, injection sites need to avoid areas of natural outflow zones which typically occur at plate boundaries (Goldberg and Slagle, 2009). This was accounted for by adding a 20 km buffer around plate boundaries. As an indicative example, with respect to the Juan da Fuca plate and using a high estimate of 40 m/year lateral flow rate taken from model-constrained estimates of zones this would equate to a 500-year buffer around potential natural outflow zones (Goldberg et al., 2008). Other areas would be expected to have different rates of hydrothermal flow; this is particularly a concern for young ocean crust which is close to active ridges. Plate boundaries (see supplementary Fig. 3) were incorporated by using data from Bird (2003) that was converted to shapefiles by Hugo Ahlenius. To obtain more accurate distance calculations, the 20 km buffer was applied during a later processing stage using appropriate universal transverse mercator (UTM) projection systems for each area.

Storage locations were also required to have 200 m sediment thickness on top of the igneous rock to act as non-permeable cap rock (Goldberg and Slagle, 2009). This was assessed using the GlobSed 5-arc-minute total sediment thickness grid (Straume et al., 2019). Using GIS, thickness data was filtered to identify areas that meet the limit (see supplementary Fig. 4). Because wells must pass through the existing sediment to reach the basalt, which implies an impact on well cost arising from differences in sediment thickness, the sediment thickness for each site was recorded for each area. In addition, there is a benefit to injecting the carbon dioxide below 2700 m water depth; at this depth the CO2 is typically heavier than water (depending on the temperature and pressure) so this may provide an additional trapping mechanism (Goldberg and Slagle, 2009). Water depth was obtained from the Global Multi-Resolution Topography (GMRT) Synthesis digital elevation model (Ryan et al., 2009) . Using GIS, water depth data was filtered to identify areas that meet the limit (see supplementary Fig. 5). This constraint was considered optional, since it is an additional failsafe that may not be required. Lastly, exclusive economic zones (EEZs, i.e. areas of the sea over which sovereign states have exclusive rights, generally extending 200 nautical miles from their shores) were identified using a dataset from the Flanders Marine Institute (Flanders Marine Institute, 2019) in order to identify which countries may be allowed to inject into any given area (see supplementary Fig. 6). Regulatory uncertainty may be greater for areas outside of any exclusive economic zone. This was also considered an optional constraint. Optional constraints were considered at a later stage as part of multiple scenarios reflecting different levels of difficulty (see Section 2.4).

2.2. Wind resources

In order to assess the distance between suitable wind resources and storage locations, wind speed at 100 m height was taken from ERA5 hourly reanalysis data at 0.25° resolution from 1986 to 2016 (Hersbach et al., 2018) and translated to 150 m using a power law with an alpha factor of 0.11. Average wind speeds were then calculated for each grid point. Particular designs of wind turbines have unique power curves that relate their power output to wind speed and wind turbines cannot operate in all conditions (Sohoni et al., 2016). The Vestas V236–15.0MW wind turbine was used as a reference (Vestas Wind Systems A/S, 2021); the reported annual energy production for one 15MW turbine is between 60GWh and 90 GWh per year for average annual mean hub-height wind speeds between 8 m/s and 11 m/s, assuming 100 % uptime; this implies a capacity factor between 46 and 68 %. Wind data was filtered to require mean wind speed greater than or equal to 8 m/s. This is sufficient to identify areas where development may be feasible but does not guarantee that there is enough wind to power all capture and storage within an area; to do so would require the application of power curves with consideration of cut-in and cut-off speeds, and would ultimately depend on the energy requirements of a full-scale offshore DAC and injection system which are not presently well understood. Currently most offshore wind farms operate at an approximate water depth limit of 200 m or less (Dvorak et al., 2010). There are however projects such as the Hywind floating platform concept targeting 1000 m depth (Elsner and Suarez, 2019). Given the large amount of energy that would likely be needed for direct air capture and the cost of energy transmission, it is assumed that the DAC device would be situated in proximity to the wind farm. Therefore, if this concept was implemented in the

short term it is expected that there would be some CO2 transportation needed between wind farms and injection locations by ship or pipeline. No restrictions were set on seabed conditions that would impact anchor designs (sand, rock, etc.). No additional restrictions were set on adding DAC or DOC to any viable wind resource, although some other site conditions such as distance to ports and shorelines are computed to understand their potential impacts on maintainability (Section 2.3). Shape files were created containing areas with viable wind speeds and water depths less than 200 m, 1000 m and unrestricted respectively (see supplementary Fig. 7). Because the distance between the centroid of a wind farm and its injection site would depend on the size of the farm and its layout, neither of which are specified here, wind farms were assumed to be sited with their first turbine as close as possible to the injection sites; the distances between the wind farm and the injection location reported in later steps should therefore be interpreted as the distance to the closest turbine, with the locations of additional turbines left to future work.

Table 1
Summary of constraints applied to scenarios.

Constraint	Scenario			
	A	B	C	D
Seismic ridge <15 MA or aseismic ridge	√	√	√	√
Sediment thickness ≥200m	√	√	√	√
20 km or further from plate boundaries	√	√	√	√
Any large port used for comparison to point-source capture	√	√	√	√
Wind speeds greater than or equal to 8 m/s at wind site	√	√	√	√
Injection and wind in same EEZ	√	√	√	
Wind area has water depth ≤1000m	√*	√*	√	
Wind area has water depth ≤200m	√	√		
Injection area has water depth ≥2700m	√			

* Constraint met implicitly due to a more extreme constraint being applied.

2.3. Ports and shorelines

Either industrial point source carbon dioxide capture or land-based DAC could be used in place of an offshore wind-powered DAC system as a competing use for ocean basalt storage, in which case marine transport would likely originate from a large port. The locations of large ports were also obtained to determine whether the storage locations were closer to viable wind areas or to ports which may allow alternate usages. The World Port Index 2019 was used to identify major ports (National Geospatial-Intelligence Agency, 2019). Ports were filtered to those whose size was classed as 'Large' in the WPI index; this classification is assigned based on area, facilities, and a variety of other factors. Port locations can be seen in supplementary Fig. 8. Unlike wind and injection sites, the use of ports is typically allowed between countries (with some notable exceptions such as the US Jones act). Consequently, when computing the distance from a storage location to the nearest port, ports were never constrained to be within the same exclusive economic zone as the country possessing the injection site. Because proximity to the shore is a geographical factor that can influence the design and operation of wind farm and CCS (carbon capture storage) projects, a shapefile of the shoreline from the North American Cartographic Information Society (Patterson and Kelso, 2012) was also used to compute distances between the shoreline and potential sites for both capture and injection. There are some minor differences between the land masses identified within the EEZ dataset and shoreline data set, with some small islands listed in the former and not the latter. However, since the primary purpose of the shoreline computation is to consider the practical maintainability of a remote system, whereas the EEZ data set considers regulatory issues, these differences are considered to be appropriate within the context of each use case.

2.4. Scenarios

To capture a range of possibilities with respect to technological and regulatory difficulties, multiple scenarios were constructed. They are summarized in Table 1. In all cases, injection sites were required to be in areas with either seismic ridges <15 million years old or aseismic ridges, and in areas with sediment thickness ≥200 m, and 20 km or further from plate boundaries. All wind areas were required to have annual mean wind speeds greater than or equal to 8 m/s. The first scenario imposed highly restrictive additional requirements, with each subsequent scenario relaxing some of the constraints.

In Scenario A, wind resources were required to be in areas with less than 200 m water depth. Both injection sites and wind sites were restricted to be within the same economic exclusive zone, and injection sites were required to be at water depth greater than 2700 m.

Although the depth constraint provides an additional storage assurance, there are technological challenges associated with operating in such deep waters. In Scenario B, injection sites were allowed to be at any water depth but all other constraints remained the same as Scenario A.

In Scenario C, wind resources were expanded to include those located in 1000 m water depth or less. No water depth limitations were applied for injection sites but both injection sites and wind sites were still restricted to be within the same EEZ. When considering the distance from a storage location to the nearest wind resource compared to that of the nearest port, the nearest large port was used even if it was in a different EEZ from the injection site.

In Scenario D all water depth limits were removed for both wind sites and injection sites. Wind sites still required mean wind speeds greater than 8 m/s. Both injection sites and wind sites could be anywhere in the ocean and injection sites could use any wind sites (and any large port when comparing the distances between storage locations and wind resources to those between storage locations and the nearest large port).

Since the constraints are progressively relaxed for each scenario, Scenario B holds all of the same area as Scenario A plus additional areas, Scenario C holds all the same areas as Scenario B plus the possibility of additional areas, and so on.

2.5. Distances between injection sites, wind resources, ports, and shore

For each scenario, all constraints other than distance to plate boundaries were first applied using GIS software (Fig. 1). For scenarios in which geographic areas were required to be within an EEZ, a label was added to each shape to indicate the EEZ in which it was found. Outside of these zones, aseismic ridges retained the name given to them in the original data set apart from some minor changes to naming and capitalization conventions in order to improve readibility. Seismic ridges were named according to a registry of undersea features if there was an area at the same geographic location. If not, they were labelled with 'Other' and the ocean in which they were found. Areas were split by their label and processed separately. Each area was first divided into UTM zones to do distance calculations with minimal projection errors. Antarctica was excluded from these calculations due to not being within any valid UTM zone, but areas just outside the UTM zone range were included using the closest matching UTM zone; this represents a very small proportion of the total area considered. Within each UTM zone, the plate boundaries were buffered by 20 km and this area was subtracted. A point grid with 20 km resolution was created within the remaining areas to represent valid injection locations. The water depth and sediment thickness at each point was recorded. The injection points were projected back to a WGS 84 projection system. A 'distance' GIS tool was used to draw lines between each injection point and the nearest edge of a wind resource area, computing the geodesic distance represented by each line. This value provides a minimum estimate of the transport distance if CO2 is captured at the wind farm and sent to the injection

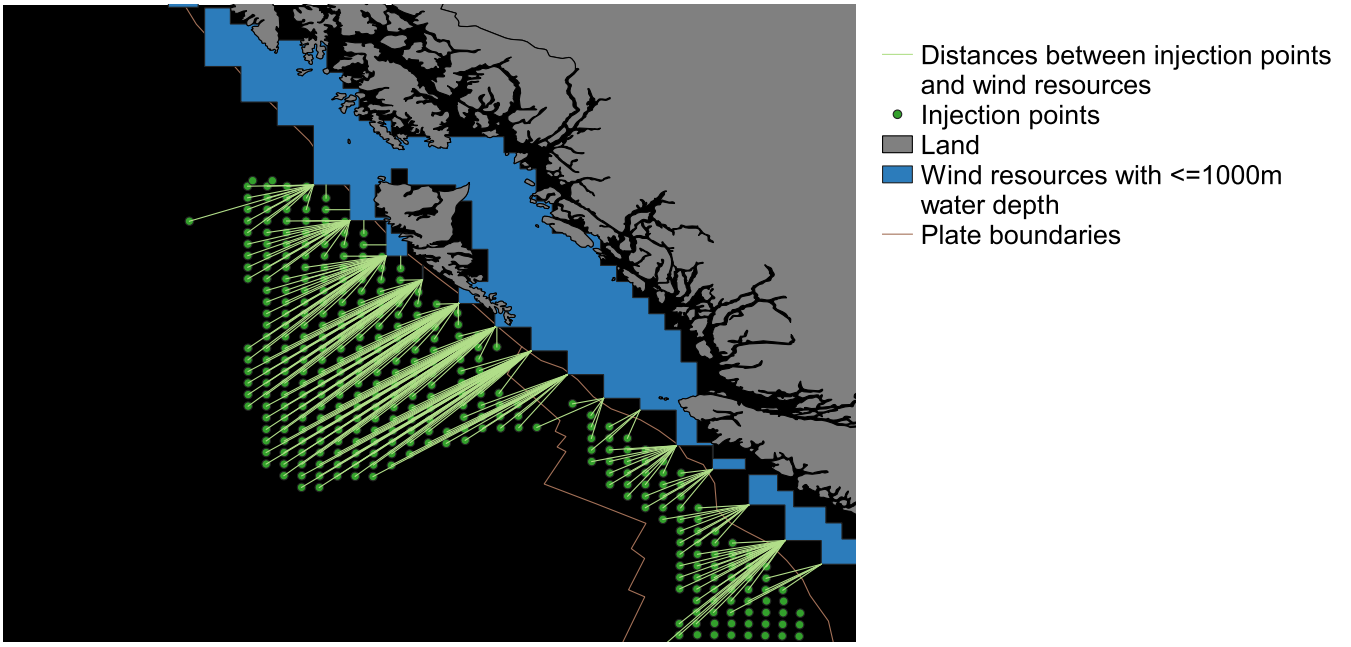

Fig. 1. Example of applying a grid and computing distances from the nearest injection point to the nearest edge of a wind resource area. The injection area shown is the Juan da Fuca plate in British Columbia, Canada with constraints from Scenario C.

location using a ship or a pipeline. The minimum value was computed because the required wind area depends on the energy requirements of the captured process, and therefore the distance to the centre of a wind resource will change depending on the underlying technological assumptions. In scenario A,B, and C only wind resource areas from the same EEZ were used. In scenario D wind resources in any area could be used. An example of this computation can be seen in Fig. 1 for the western coast of Canada. The distance between each identified edge of the wind resource and shore was also calculated by using an 'endpoint' GIS process to make a point at the end of each distance line, then using the distance process again to compute the line between this new endpoint and the vectors deliniating the shoreline. The same distance routine was used to compute the distances between the original injection points and the nearest major port; this was used later on to determine what percentage of the potential storage sites identified were closer to a large port than a wind resource. Costs for offshore CO2 transport were estimated from (ZEP, 2011a) (converted to USD using exchange rates from (Bank of Canada, 2017) and modified for a 2021 basis using the upstream capital cost index (IHS Markit, 2022) for an overall adjustment of 1.18 2021USD/2011 EURO) in order to estimate the resulting CO2 transportation cost implied by the resulting distances. The distance between the original injection points to shore was also computed for informational purposes, because the distance to shore would have implications for the operation and mainetance of any proposed CO2 storage project.

2.6. Storage capacities

To estimate total storage capacity the available pore volume was estimated and then multiplied by the density of CO2. Given that each grid point was 20 km away from its nearest neighbour on all sides, it represented a 20 km by 20 km square and therefore 400km2 area. Storage locations were assumed to have 10 % porosity within the basalt (Goldberg and Slagle, 2009). The porous area was taken to extend between 20 and 100 m in thickness; the capacity was calculated separately for 20 m and 100 m to yield a minimum and maximum range. Assuming that the CO2 is injected in a liquified state (which has a density of approximately 1 g CO2/m3) and is fixed as CaCO3 (0.36 g C/m3 with two O2 molecules also originating from the CO2 for each molecule of carbon (Goldberg and Slagle, 2009)), each porous volume was estimated to be able to hold ~1 g CO2/m3 (Goldberg and Slagle, 2009). The total capacity for each scenario was aggregated globally. For Scenarios A to C, since injection sites and wind sites were required to be in the same EEZs, injection sites were then filtered to exclude EEZs with no available wind resources and the remaining capacity calculated. Injection sites were then filtered again to exclude any areas where a major port is closer than the nearest wind resource within their respective EEZ (presuming that they may be used for point source or land-based capture) and the remaining capacity calculated. Being closer to a wind resource does not necessarily imply that it would be cheaper to use an offshore system; although CO2 transportation costs would be minimized, the cost and performance of offshore capture would be different from an onshore system, for example due to additional costs to equip the capture system for the more extreme offshore conditions and provide access for ongoing operations and maintenance. In practice these costs would be difficult to calculate at a global scale. This calculation is simply indicative of the proximities involved.

2.7. Additional features of potential storage locations

For each scenario, the available capacity was separated into bins based on the distance between the wind resource and the storage location, and the results displayed for each EEZ (or for the nearest ridge name for areas outside of an EEZ). Scenario C, a 'middle of the road' scenario, was then selected for more detailed analysis:

- Injection locations were colour-coded based on distance to wind resources and plotted (Figs. 2b, 3).
- Injection locations were ordered in ascending order of distance to wind resources and the cumulative capacity was plotted with estimated transportation cost as a secondary axis (Fig. 4a).
- Injection locations were ordered by distance to the nearest large port and plotted with estimated transportation cost as a secondary axis (Fig. 4b).
- For each injection location, the closest location within an area of acceptable wind resource was identified, i.e. the nearest wind location. These nearest wind locations were then sorted by their distance to

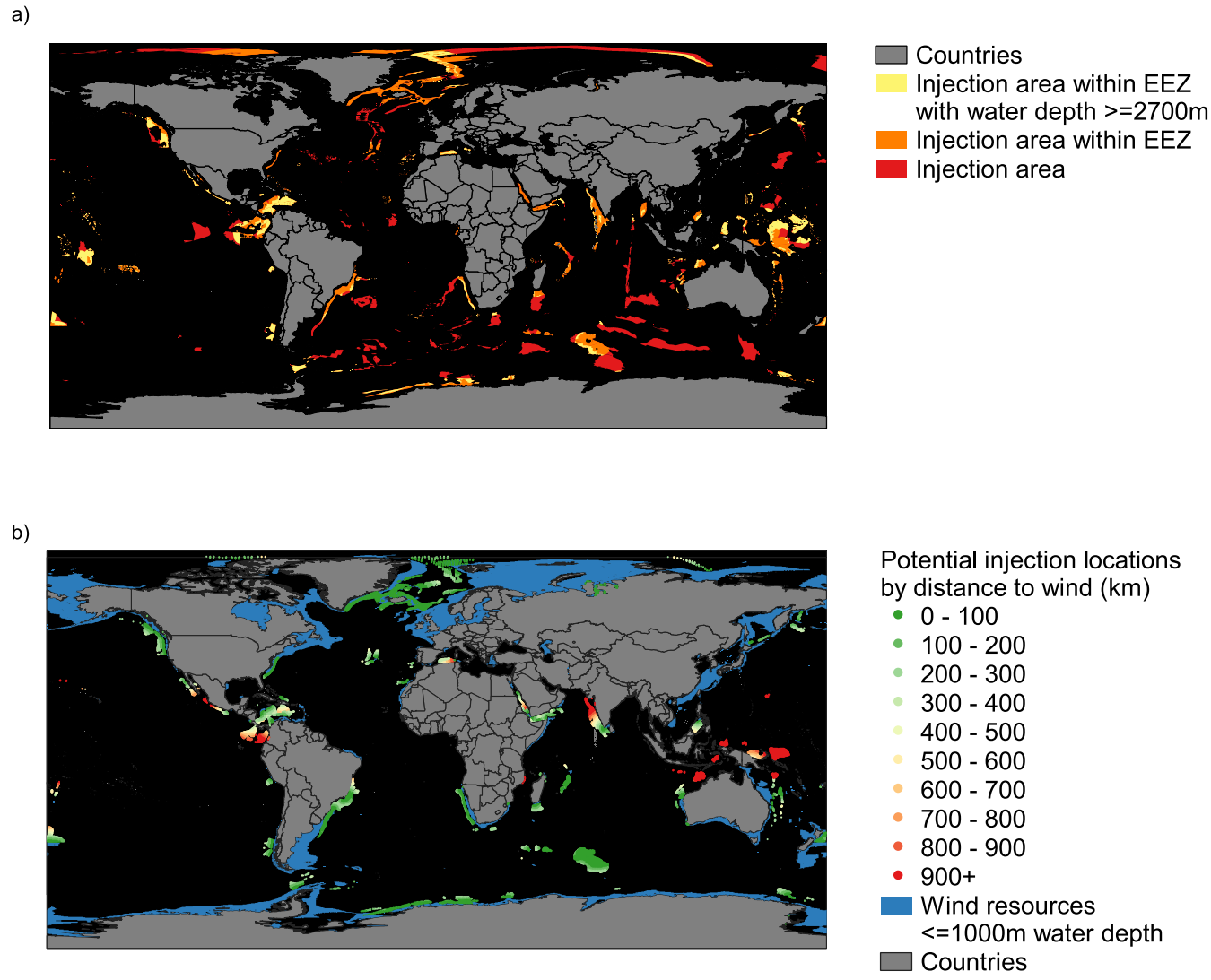

Fig. 2. a) Areas within EEZs with water depths less than or equal to 2700 m (Scenario A), injection areas within an EEZ (Scenarios B and C), and injection areas anywhere around the world (Scenario D). The constraints are progressively relaxed. As a result, Scenario B holds all the same area as Scenario A plus additional areas which did not meet Scenario A's constraints, etc. b) Injection locations for scenario C colour coordinated by distance to wind resources.

shore, and a cumulative distribution of distance to shore was computed and plotted (Fig. 5).
- Injection locations were ordered by water depth and plotted (Fig. 6a).
- Injection locations were ordered by sediment thickness and plotted (Fig. 6b).
- Injection locations were binned by distance to shore and water depth. The results were plotted as a heat map (Fig. 7).

3. Results

3.1. Global capacity estimates and sensitivity to technological and regulatory challenges

The potential injection areas represent vast storage capacities (see Table 2) ranging from 9900 to 196,000Gt depending on the applied constraints. Relaxing the constraints increases the available sequestration capacity by a factor of approximately 10. The only constraints that made very little difference was the wind resource water depth between Scenario B (requiring wind resources in water depth less than 200 m) and Scenario C (requiring wind resources in water depth less than 1000 m). This implies that currently commercial floating wind technology would be sufficient in the near term, because most areas with 1000 m depth wind have at least a small amount of wind resources that is within 200 m.

3.2. Most promising locations and site-specific parameters

Moving from more constrained to less constrained scenarios, there are approximately 45–80 countries with at least some ocean basalt sequestration capacity compared to the roughly 230 EEZ within the original data set (20–35 %). Scenario A identified locations primarily off the coast of the United States and around the equator (supplementary Fig. 9), while notable new areas included in Scenario C and D were off the coast of India, Brazil, and Greenland. While roughly half of the capacity was found in international waters in Scenario D (see Table 2), up to 106,000 GtCO2 of capacity is still available within EEZs which suggests that it may not be necessary to go outside of EEZs. However, there are some large areas in the Indian Ocean which look very promising given their large capacities (see figure supplementary Fig. 12). Considering the middle-of-the-road scenario, Scenario C, estimated capacity ranged from 21,000–106,000Gt with roughly half of available injection areas

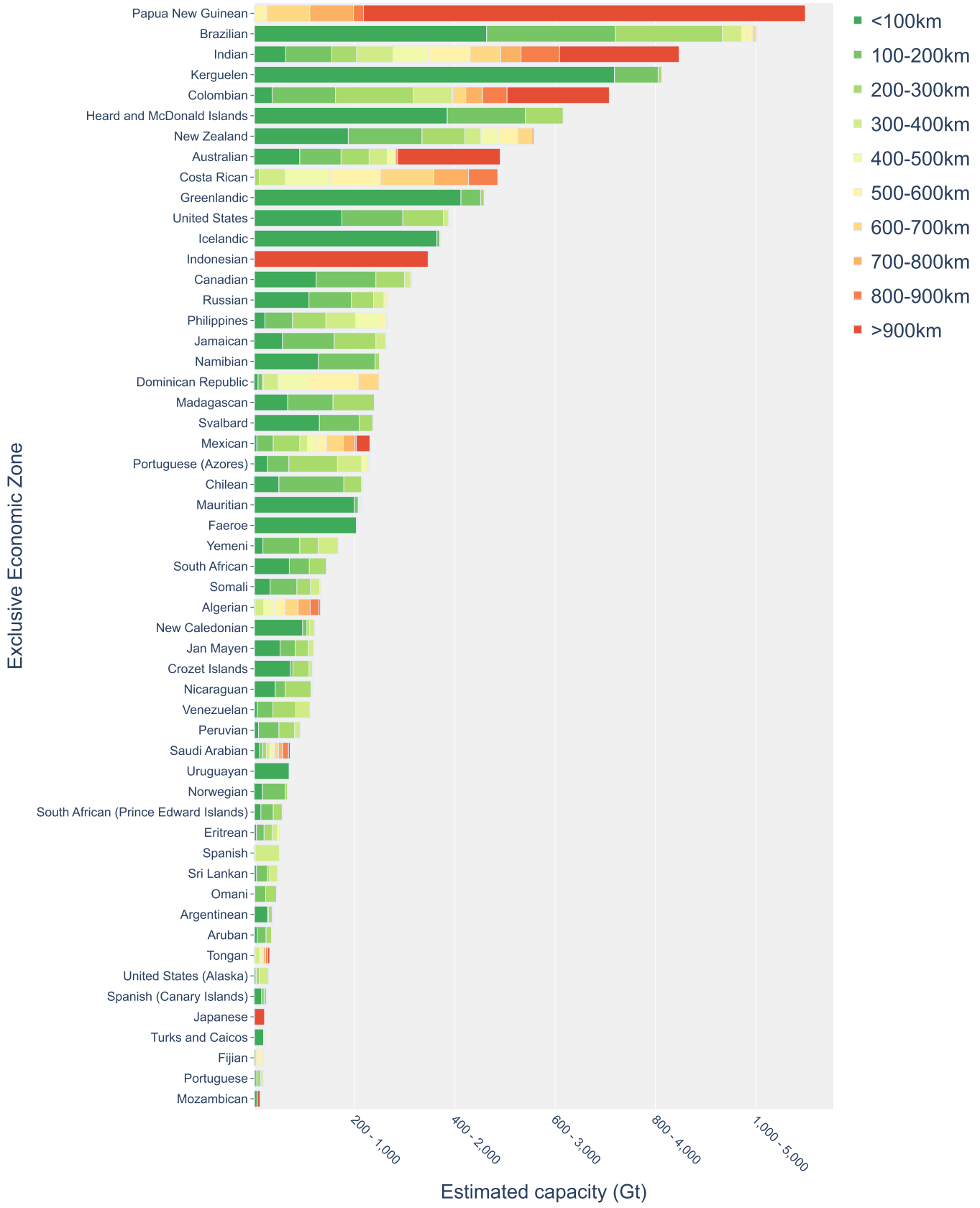

Fig. 3. Scenario C largest areas of potential ocean basalt carbon sequestration sites per country and distances to wind resources within the same exclusive economic zone. The range of storage capacity estimates reflect porous basalt areas that extend between 20 m (lower estimate) and 100 m (higher estimate) . Areas with minimum capacity < 10Gt were excluded.

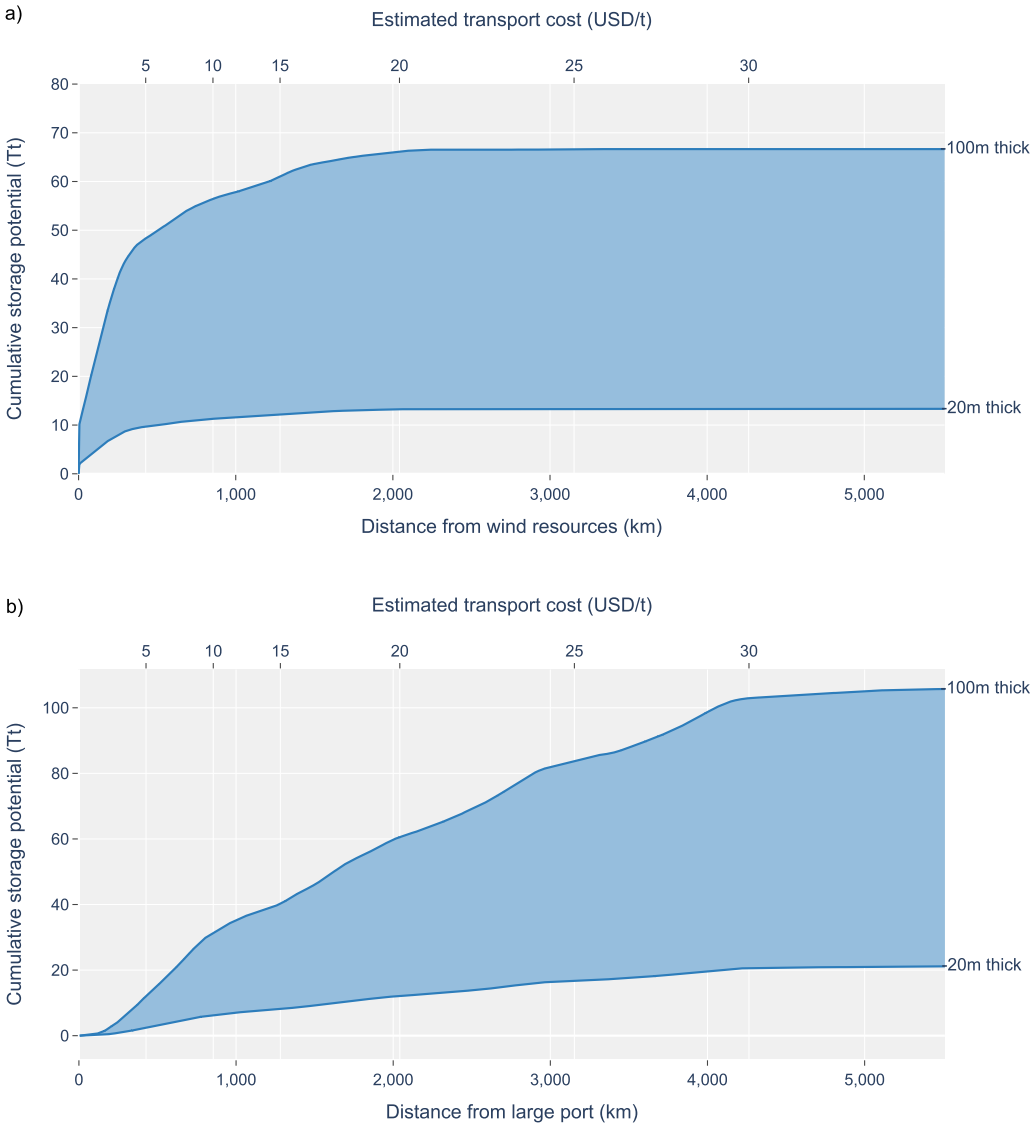

Fig. 4. Cumulative injection capacity (in Teratonnes) meeting constraints of Scenario C, ordered by transport distance to nearest wind resources (a) and nearest large port (b). Costs for offshore CO2 transport were estimated from ZEP (2011a) and converted to USD using exchange rates from Bank of Canada (2017); the scale is non-linear due to more efficient use of capital investments and different types of transport over longer distances. The range of storage capacity estimates shown reflect porous basalt areas that extend between 20 m (lower estimate) and 100 m (higher estimate) below the ocean sediment.

Table 2
Capacity estimates for technological and regulatory challenge scenarios (Gt CO2).

Scenario	Total potential CO2 storage capacity	CO2 storage capacity located within same EEZ as a suitable wind resource if applicable	CO2 storage capacity closer to a wind resource than to a large port
A	9900 - 49,200	4300 - 22,000	3800 – 19,000
B	21,000 - 106,000	12,000 – 62,000	11,000 –55,000
C	21,000 - 106,000	13,000 - 67,000	12,000 - 61,000
D – Inside EEZ	21,000 – 106,000	21,000 – 106,000	20,000 – 98,000
D – Outside EEZ	18,000 – 90,000	18,000 – 90,000	18,000 – 90,000

for each scenario found within the same EEZ as a suitable wind resource (see Table 2). Most of these areas were also within 1000 km of a suitable wind resource (see Fig. 4) and closer to the wind resources than to any major ports (see Table 2). Typically, the best areas were found far from the equator due to the greater prevalence of good wind resources in those areas (see Fig. 2b). Some potential hotspots for deployment of offshore wind-powered CDR include the east coast of Latin America (Brazil, Columbia), the west coast of North America (the United States, Canada), Australasia (Australia, New Zealand) some northern arctic countries (Iceland, Greenland), and some subantarctic islands (Kerguelen Island, Head and MacDonald Islands). Thirty EEZ's alone contained most of the available capacity (Fig. 3). Twelve of these thirty zones belonged to G20 countries, and two to G7 countries (Canada and the US). However, there are large differences in capacity between countries with

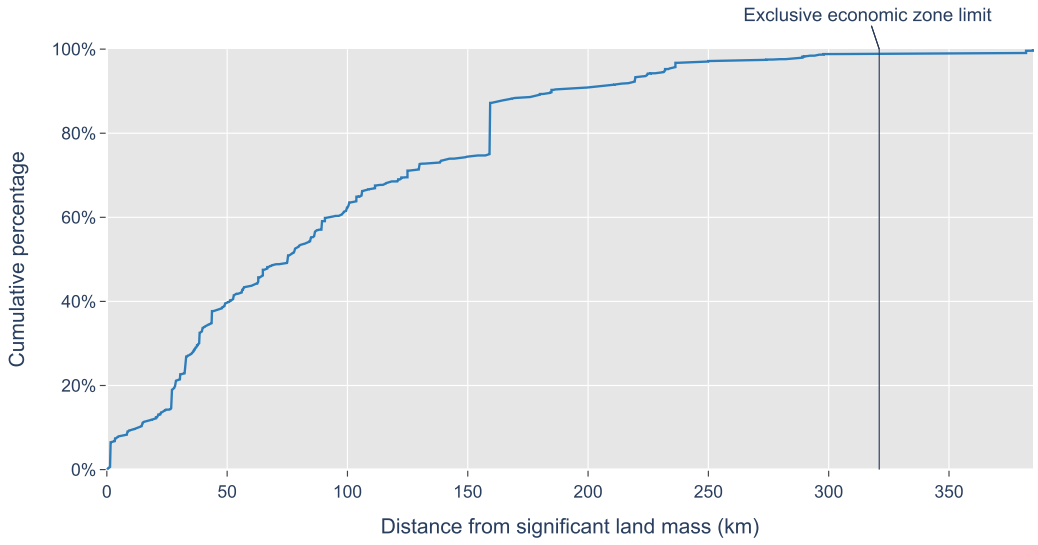

Fig. 5. Cumulative distribution of distance to a significant land mass for the nearest wind location for each injection location in Scenario C. Only areas within EEZs which contained viable wind resources are included. Note that distances significantly in excess of 321 km (200 nautical miles) are typically areas near small islands whose shoreline is not included in the shoreline dataset from which significant land masses are derived.

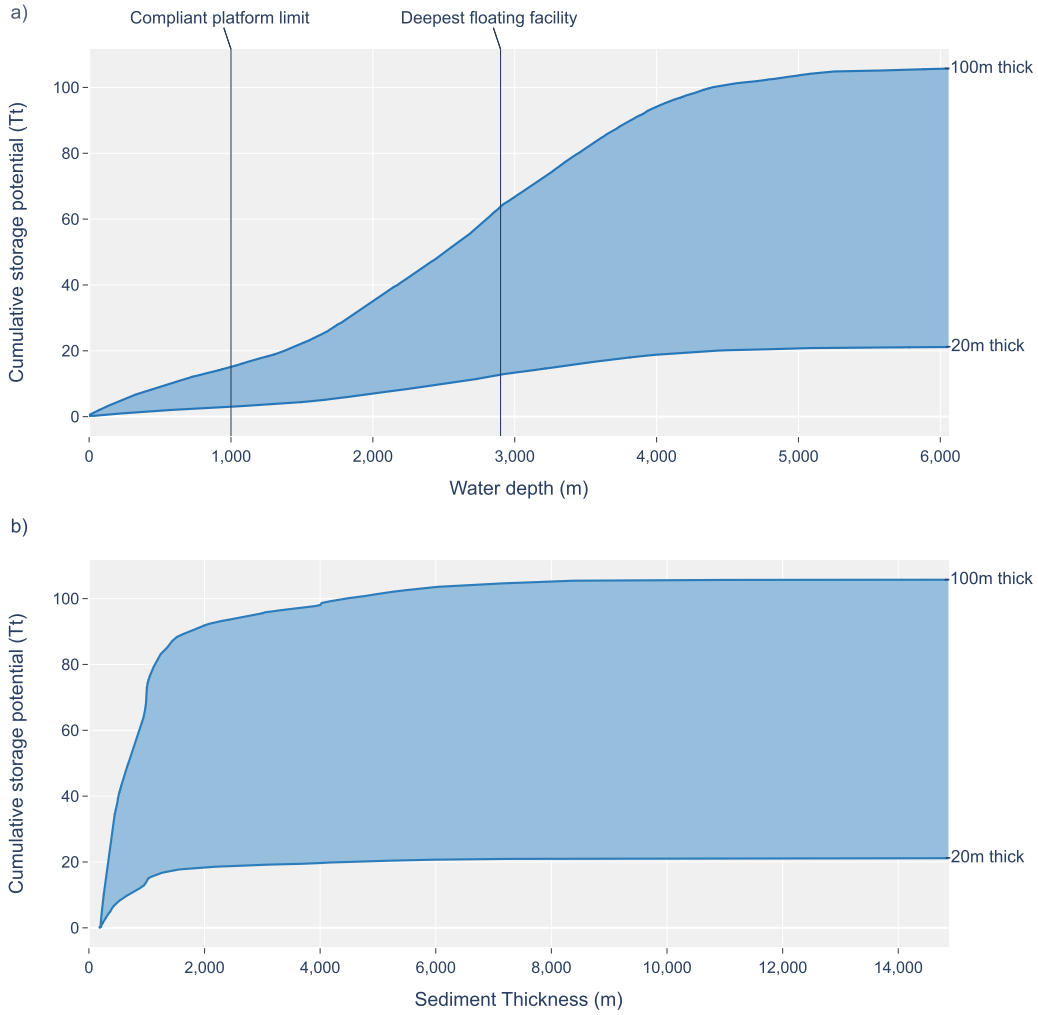

Fig. 6. Cumulative injection capacity (in Teratonnes) meeting constraints of Scenario C ordered by water depth (a) and sediment thickness (b). All areas are included irrespective of proximity to wind resources. The range of storage capacity estimates shown reflect porous basalt areas that extend between 20 m (lower estimate) and 100 m (higher estimate) below the ocean sediment. The approximate water depth limit at which compliant tower platforms become un-economical (da Ponte Jr, 2021) is noted, because they are a type of fixed platform that can be used in relatively deep water. The water depth of the Stones project (Webb and Vugt, 2017) is also noted, since it is the deepest oil and gas project at the time of writing.

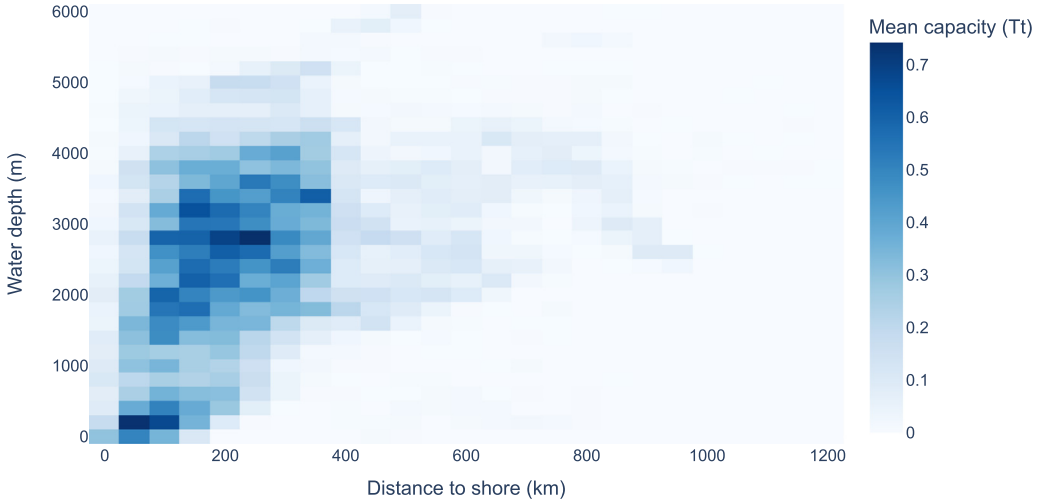

Fig. 7. Heat map of potential capacity of injection sites meeting constraints of Scenario C binned by water depth and distance to nearest significant land mass. Sites that are further than 1500 km from shore are excluded because their capacity is too small to be visible on the heat map (this represents much less than 1 % of all sites). The capacity estimates shown reflect porous basalt areas that extend 60 m below the ocean sediment (the mean of the higher and lower estimates).

potential storage locations (see Fig. 3), with the top 10 countries having estimated potential of at least 400–2000 Gt compared to less than 20–100Gt for the bottom 10 (and of course many others with none at all). In scenario C, the majority of injection areas were found within 500 km of wind resources (Fig. 4a), with small numbers of sites being identified with increasingly long distances. Distance to a large port was more evenly distributed between 200–4000 km (Fig. 4b). Most of the wind resources closest to the injection sites were found within 150 km of shore. Since all locations in Scenario C for both injection and wind are within an EEZ, they would normally be expected to be within 200 nautical miles (approximately 320 km); the small number of injection and wind sites outside of this range resulted primarily from small differences in the EEZ and shoreline data sets (see Section 2.3). Water depths ranged widely for the injection locations, from very nearly onshore to greater than 6000 m depth (Fig. 6a). Although sediment thickness can exceed 14,000 m in rare cases, most sites had sediment thickness of less than 2000 m (Fig. 6b). Areas that are further from shore are more likely to be situated in greater water depths (Fig. 7). Partially as a result, and partially due to the large amount of global potential, areas can be identified that are both in shallow water and close to shore (Fig. 7); for example, some of these areas can be found in Brazil, the United States, and Iceland.

4. Discussion

4.1. Drivers and implications of global capacity estimates

This study identified many of the same areas as shown by Pilorgé et al. (2021) such as in Brazil and Iceland, but highlights a number of new areas such as off the coast of Canada and Australia. These differences likely arise because Pilorgé et al. reported on areas that were directly co-located between offshore wind and basalt, whereas this study allowed for a range of distances. The 4,300Gt to 196,000Gt reported in this study reflects a wider range of values than the 8238 – 41,191Gt reported by Goldberg and Slagle (2009). This is expected because this paper uses multiple scenarios, the most conservative of which is more restrictive than their assumptions (the constraints in Scenario A are similar to their paper but we consider only areas within an EEZ with offshore wind availability) and the most relaxed of which is more expansive than their assumptions (in Scenario D we relax the requirement for deep water, and consider the entire globe rather than restricting to particular areas that they used in their paper). Both studies agree that there is substantial potential capacity for carbon dioxide sequestration in subsea basalt.

The total area available for injection once all constraints are imposed is much less than the total area containing seismic ridges < 15Ma and aseismic ridges (see Fig. 2a in comparison to supplementary Figs. 1 and 2). This can be explained partially because most of the original area consisted of seismic ridges, and the constraints imposed upon seismic ridges are not independent of one another. For example, fast spreading ridges like the East Pacific Rise on the left-hand side of supplementary Fig. 1 naturally create large parallel, adjacent swaths of crust with the same age resulting in large areas which meet the age constraint. However, these younger seismic ridge areas with high porosity are less likely to have high sediment thickness because there has been less time for sediment to accumulate, so that does not translate into greater injection areas within this region in Fig. 2a. However, even the most conservative cumulative estimate of 4,300Gt potential storage is multiple orders of magnitude greater than that required to support the roughly 10 Gt/year of negative emissions technologies which is estimated to be required by 2050 and 20 Gt/year required by 2090 (NASEM, 2019). On the other hand, total cumulative potential capacity is not equivalent to the total capacity that would meet all requirements for a project in practice. For this potential capacity to be utilized it must be possible to inject into it within a reasonable timeframe; this depends on both the permeability of the basalt and the number of injection wells which can be built within a reasonable cost and time. In other offshore carbon capture and storage projects, it is often expected that multiple areas will undergo injection tests before a suitable location is found (ZEP, 2011b), and there is no reason to believe that ocean basalt would be any different. Further requirements that might be expected of an ocean basalt storage site include confirmation of porosity and permeability via a test well, a more detailed demonstration of an impermeable sedimentary cover across a sufficiently wide area with a seismic survey, etc. (see Alcalde et al. 2021) for a more complete screening process). Further, the presence of a nearby ‘high quality’ wind resource does not guarantee that enough windy areas exist to power a CDR system that can use all available storage over a reasonable time period. This is of greatest concern in Scenario A, since the other scenarios identified very large areas of potential wind resources (see supplementary Fig. 7). The energy requirements for carbon dioxide capture vary depending on the capture method (Digdaya et al., 2020) and are changing rapidly with the emergence of new electrochemical methods for seawater and direct air capture (for example, see Kim et al. (2023) and Xu et al. (2023)).

Conducting a more detailed study on some of the hotspots identified by this reearch to assess the capacity of both offshore wind and storage at those locations, in consideration of both present conditions and predicted climate change impacts, is suggested as future work. Regardless, the sheer magnitude of candidate locations is very promising, and having many areas with high potential storage capacity may make it possible to prioritize locations which have the best attributes to reduce the overall cost of the system such as shallow water depth or proximity to shore.

Due to the uneven distribution of potentially suitable locations globally, if the proposed concept for offshore capture with ocean basalt storage systems did come to fruition, it may be lead by a minority of countries who possess the areas with the most favourable attributes and who may then redistribute verified carbon offsets to those who do not. Therefore, the existence of policies that allow countries to fund carbon dioxide removal projects in other countries and received verified carbon credits in order to meet their own emissions reductions targets would be beneficial to support these types of projects. The countries with potential storage capacity include a mix of high income nations (e.g. USA, Australia, Canada), less high income nations (e.g. Brazil, Namibia), and relatively small remote colonies or territories (e.g. Kerguelen Islands, Head and McDonald Islands). This implies that there are a number of geopolitical contexts in which ocean basalt storage sites may be developed, for example funded directly by higher income nations in their own countries or as part of responsible economic development initiatives elsewhere in the world.

4.2. Implications of water depths, sediment thicknesses, and distances between injection points, wind resources, ports, and shores

The proximity between wind resources and injection locations suggests that in many cases there may be some value in attempting air or ocean capture close to offshore basalt storage rather than using the potential storage locations for point source capture and storage. However, there are other considerations. For example, point-source carbon capture may be significantly cheaper, but point source capture acts to avoid future emissions rather than removing past emissions. Onshore capture may also be cheaper at further distances but is subject to land availability and competition for renewable resources with onshore energy uses. Depending on the type of capture, there may be other issues: for example, detractors of bioenergy with carbon capture and storage argue that it risks competition for food resources, adverse impacts on rural communities, and biodiversity loss (Sandalow et al., 2021). More detailed cost-benefit analyses are suggested for future work. What is clear is that compared to the 10–20Gt/year estimated requirements for NETs in the 21st century, there is very high potential capacity within close proximity to ports, shores, and wind resources. This suggests that it may ultimately be practical to use ocean basalt storage for all of the above uses. Similarly, the distance to a nearby port also has implications for the construction, operation, and maintenance of offshore wind farms along with capture and injection systems. In practice, there is a trade-off between avoiding competition with other energy uses and incurring additional costs. There is a similar trade-off between locations at shallower water depths which can benefit from less expensive types of drill ships, offshore platforms, etc., and the younger basalt found in deep water close to plate boundaries which may have higher porosity and permeability. While increased sediment thickness may reduce the risk of a leakage, it also increases the depth of the wells that are necessary for CO2 injection. What this study shows (particularly Figs. 4–6) is that vast potential exists at site conditions in which pre-existing offshore wind and oil and gas technologies operate or are targeting. Therefore, technological development efforts may wish to focus on the development and scaling up of offshore air or seawater capture technologies, as well as adaptation of pre-existing transport and injection technologies for subsea basalt.

4.3. Future development of offshore wind-powered CDR with ocean basalt sequestration

There are multiple important outstanding questions with respect to this technological concept. Firstly, there are not many areas for which the ocean basalt has been well characterized; this creates uncertainty with respect to global injectivity, porosity, hydrothermal flow, and carbonation estimates which are needed to fully assess this technology. More comprehensive offshore drilling and detailed modelling efforts are recommended to reduce the uncertainty in these estimates, backed by further laboratory or injection test results to understand the implications of geological differences on CO2 flow and mineralization reactions. Given the prevalence of co-located wind and potential storage locations generally towards the poles, efforts to assess marinization of DAC or ocean capture and its integration into offshore wind turbines may wish to focus on the conditions typically experienced by those two general areas. It is also worth noting that many of the potential storage areas that are closest to shore (e.g. in Brazil, Columbia, New Zealand, Australia, and South Africa) originate from Large Igneous Provinces rather than seismic ridges. This is likely due to many seismic areas that are closer to shore failing to meet the age restriction that was imposed to help ensure porosity and permeability. Considering that, offshore drilling and modelling efforts would ideally make sure to include Large Igneous Provinces.

In general, carbon dioxide storage in basalt/ultra-mafic rocks has only been rated at technological readiness level 2–6 (Kearns, 2021) and, to our knowledge, offshore basalt storage has never been done before. Even if it is possible, it may not be economic. In addition, because of dissolution and reactive transport that occurs when injecting carbon dioxide into basalt, conventional monitoring solutions for carbon dioxide plumes are not suitable for this type of rock (Kearns, 2021). The Carbfix project in the past has used injected tracers with numerous monitoring wells for characterisation and monitoring (Matter et al., 2009), but offshore wells are very expensive compared to onshore wells. DAC technology is maturing quickly, but, to our knowledge, DAC has never been performed offshore; current technological designs may not be suitable in the salty and high-motion conditions. Laboratory scale tests that mimic offshore conditions may be beneficial to quantify the implications of offshore conditions. Since many of the locations identified are further from shore and potentially subject to more extreme conditions, operations and maintenance may be a challenge. The offshore climate may also exceed the operating temperature range of DAC units (this is also a consideration onshore (Sendi et al., 2022)). There is therefore no guarantee that an area with storage capacity and proximity to a wind resource will be technologically or financially viable until these outstanding questions are resolved. In addition, the ultimate viability of these systems relates not only to their own performance, but also how they compare to alternative uses for the same wind energy such as hydrogen production or ocean alkalinity enhancement. Social license to operate is also necessary; although a recent study found majority support for one particular implementation of offshore-wind powered CDR using direct air capture and storage into ocean basalt, sometimes all that it takes is a single negative event to generate strong negative reactions and wider mistrust (Satterfield et al., 2023). Presently there are also substantial economic challenges to the implementation of carbon dioxide capture from air and seawater even when conducted onshore and using renewable electricity that is cheaper than would be expected for offshore wind (Eisaman et al., 2018; Young et al., 2023). What is clear is that further technological, economic, and social progress would be needed to attain repaid deployment of this technological concept.

5. Conclusion

There are numerous areas situated around the world which meet the preliminary requirements for situating an offshore wind powered CDR system with injection into ocean basalt rock, most of which are

situated near the poles. Total potential storage capacity within reach of wind resources is estimated to be between 38,000–196,000Gt depending on uncertainties in porosity, with potential capacity reducing down to 4,300–22,000Gt as additional constraints are imposed. Even the most conservative estimates represent enormous capacity compared to global targets for negative emissions technologies. Most of the areas which are suitable for this technological concept are located within the EEZs of a small number of countries. Countries with considerable capacities close to wind resources when considering scenarios with relatively strict requirements include: Columbia, New Zealand, the United States, Canada, Brazil, the Kerguelen Islands, and Australia. Vast potential capacities exist within water depths, shore distances, and transport distances that are commonly found in offshore projects within other industries. The identified hotspots and site conditions may be used to: site pilot tests in order to inform essential performance parameters such as ocean basalt injectivity and offshore operations and maintenance requirements for DAC and/or DOC; inform modelling efforts for life-cycle costs and emissions of the proposed concepts coupling offshore wind-powered carbon dioxide removal with ocean basalt sequestration; and eventually target the most promosing locations for commercial storage projects.

Declaration of competing interest

The authors declare that they have no known competing financial interests or personal relationships that could have appeared to influence the work reported in this paper.

CRediT authorship contribution statement

Heather Norton: Conceptualization, Data curation, Formal analysis, Methodology, Writing – original draft, Writing – review & editing, Software, Validation. **Devin Todd:** Conceptualization, Supervision, Writing – review & editing. **Curran Crawford:** Conceptualization, Supervision, Writing – review & editing, Funding acquisition.

Acknowledgments

Funding: The authors acknowledge the support from the Pacific Institute for Climate Solutions for the Solid Carbon partnership and Private donor funding.

Supplementary materials

Supplementary material associated with this article can be found, in the online version, at doi:10.1016/j.ccst.2024.100231.

References

Alcalde, J., Heinemann, N., James, A., Bond, C.E., Ghanbari, S., Mackay, E.J., Haszeldine, R.S., Faulkner, D.R., Worden, R.H., Allen, M.J., 2021. A criteria-driven approach to the CO2 storage site selection of East Mey for the acorn project in the North Sea. Mar. Pet. Geol. 133, 105309. doi:10.1016/j.marpetgeo.2021.105309.

Awolayo, A.N., Laureijs, C.T., Byng, J., Luhmann, A.J., Lauer, R., Tutolo, B.M., 2022. Mineral surface area accessibility and sensitivity constraints on carbon mineralization in basaltic aquifers. Geochim. Cosmochim. Acta 334, 293–315. doi:10.1016/j.gca.2022.08.011.

Bank of Canada, 2017. Historical noon and closing rates [WWW Document]. Historical Noon and Closing Rates - Bank of Canada. URL https://www.bankofcanada.ca/rates/exchange/legacy-noon-and-closing-rates/(accessed 2.17.21)

Bird, P., 2003. An updated digital model of plate boundaries. Geochem. Geophys. Geosyst. 4. doi:10.1029/2001GC000252.

Captura, 2023a. Captura's 100-ton Carbon Removal System to be Installed at AltaSea at the Port of Los Angeles [WWW Document]. Captura. https://capturacorp.com/capturas-100ton-carbon-removal-system-to-be-installed-at-altasea-at-the-port-of-los-angeles/ (accessed 2.21.24).

Captura, 2023b. Captura and Deep Sky Partner to Fight Climate Change by Deploying Ocean Carbon Removal in Canada [WWW Document]. Captura. https://capturacorp.com/captura-and-deep-sky-partner-to-fight-climate-change-by-deploying-ocean-carbon-removal-in-canada/ (accessed 2.21.24).

Carbfix, 2022. Tenfold increase to CO2 direct air capture and storage at Hellisheiði - Carbfix [WWW Document]. URL https://www.carbfix.com/the-new-plant-called-mammoth-increases-the-direct (accessed 8.3.23)

Carbon Engineering, 2023. The story behind carbon engineering [WWW Document]. Carbon Engineering. https://carbonengineering.com/our-story/(accessed 8.3.23).

Chadwick, R.A., Eiken, O., 2013. Offshore CO2 storage: sleipner natural gas field beneath the North Sea. Geological Storage of Carbon Dioxide (Co 2): Geoscience, Technologies, Environmental Aspects and Legal Frameworks in: Gluyas, J., Mathias, S. (Eds.). Woodhead Publ Ltd, Cambridge 227-+ doi:10.1533/9780857097279.3.227.

Clark, D.E., Oelkers, E.H., Gunnarsson, I., Sigfússon, B., Snæbjörnsdóttir, S.Ó., Aradóttir, E.S., Gíslason, S.R., 2020. CarbFix2: CO2 and H2S mineralization during 3.5 years of continuous injection into basaltic rocks at more than 250 °C. Geochim. Cosmochim. Acta 279, 45–66. doi:10.1016/j.gca.2020.03.039.

Orca - the world's first large-scale direct air capture and storage plant 2021 [WWW Document]. URL https://climeworks.com/orca (accessed 10.13.21)

Coffin, M., Duncan, R., Eldholm, O., Fitton, J.G., Frey, F., Larsen, H.C., Mahoney, J., Saunders, A., Schlich, R., Wallace, P., 2006. Large igneous provinces and scientific ocean drilling: status quo and a look ahead. Oceanography 19, 150–160. doi:10.5670/oceanog.2006.13.

da Ponte Jr, G.P., 2021. Risk Management in the Oil and Gas Industry. Gulf Professional Publishing doi:10.1016/B978-0-12-823533-1.00015-0.

Digdaya, I.A., Sullivan, I., Lin, M., Han, L., Cheng, W.H., Atwater, H.A., Xiang, C., 2020. A direct coupled electrochemical system for capture and conversion of CO2 from oceanwater. Nat. Commun. 11, 4412. doi:10.1038/s41467-020-18232-y.

Dvorak, M.J., Archer, C.L., Jacobson, M.Z., 2010. California offshore wind energy potential. Renew. Energy 35, 1244–1254. doi:10.1016/j.renene.2009.11.022.

Edwards, E.C., Holcombe, A., Brown, S., Ransley, E., Hann, M., Greaves, D., 2023. Evolution of floating offshore wind platforms: a review of at-sea devices. Renew. Sustain. Energy Rev. 183, 113416. doi:10.1016/j.rser.2023.113416.

Eisaman, M.D., Rivest, J.L.B., Karnitz, S.D., de Lannoy, C.F., Jose, A., DeVaul, R.W., Hannun, K., 2018. Indirect ocean capture of atmospheric CO2: part II. Understanding the cost of negative emissions. Int. J. Greenh. Gas Control 70, 254–261. doi:10.1016/j.ijggc.2018.02.020.

Ekpo Johnson, E., Scherwath, M., Moran, K., Dosso, S.E., Rohr, K.M., 2023. Fault slip tendency analysis for a deep-sea basalt CO2 injection in the cascadia basin. GeoHazards 4, 121–135. doi:10.3390/geohazards4020008.

Elsner, P., Suarez, S., 2019. Renewable energy from the high seas: geo-spatial modelling of resource potential and legal implications for developing offshore wind projects beyond the national jurisdiction of coastal States. Energy Policy 128, 919–929. doi:10.1016/j.enpol.2019.01.064.

Flanders Marine Institute, 2019. Maritime boundaries geodatabase: maritime boundaries and exclusive economic zones (200NM), version 11.

Foxall, R., Ishaq, H., Crawford, C., 2023. Ambient wind conditions impact on energy requirements of an offshore direct air capture plant.

Foxall, R., Ishaq, H., Crawford, C., 2023. Marinisation for offshore direct air capture–design evaluation for air pre-treatment to remove aerosolized salt particles.

Foxall, R., 2023. Prospects for direct air capture onboard floating offshore wind turbines (Thesis).

Fuss, S., Lamb, W.F., Callaghan, M.W., Hilaire, J., Creutzig, F., Amann, T., Beringer, T., de Oliveira Garcia, W., Hartmann, J., Khanna, T., Luderer, G., Nemet, G.F., Rogelj, J., Smith, P., Vicente, J.L.V., Wilcox, J., del Mar Zamora Dominguez, M., Minx, J.C., 2018. Negative emissions–Part 2: costs, potentials and side effects. Environ. Res. Lett. 13, 063002. doi:10.1088/1748-9326/aabf9f.

Goldberg, D., Slagle, A.L., 2009. A global assessment of deep-sea basalt sites for carbon sequestration. Energy Procedia Greenh. Gas Control Technol. 9 1, 3675–3682. doi:10.1016/j.egypro.2009.02.165.

Goldberg, D.S., Takahashi, T., Slagle, A.L., 2008. Carbon dioxide sequestration in deep-sea basalt. Proc. Natl. Acad. Sci. 105, 9920–9925. doi:10.1073/pnas.0804397105.

Goldberg, D.S., Lackner, K.S., Han, P., Slagle, A.L., Wang, T., 2013. Co-location of air capture, subseafloor CO2 sequestration, and energy production on the Kerguelen Plateau. Environ. Sci. Technol. 47, 7521–7529. doi:10.1021/es401531y.

Goldberg, D., Aston, L., Bonneville, A., Demirkanli, I., Evans, C., Fisher, A., Garcia, H., Gerrard, M., Heesemann, M., Hnottavange-Telleen, K., Hsu, E., Malinverno, C., Moran, K., Park, A.H.A., Scherwath, M., Slagle, A., Stute, M., Weathers, T., Webb, R., White, M., White, S., 2018a. Geological storage of CO2 in sub-seafloor basalt: the CarbonSAFE pre-feasibility study offshore Washington State and British Columbia. In: Proceedings of the Energy Procedia, Carbon in natural and engineered processes: Selected contributions from the 2018 International Carbon Conference, 146, pp. 158–165. doi:10.1016/j.egypro.2018.07.020.

Goldberg, D., Bonneville, A., Stute, M., Fisher, A., Park, A.H., Gerrard, M., Moran, K., Hnottavange-Telleen, K., Slagle, A., Demirkanli, I., White, M., Scherwath, M., Heesemann, M., Aston, L., Webb, R., Hsu, E., Evans, C., Zahn, L., 2018b. Integrated Pre-Feasibility Study for CO2 Geological Storage in the Cascadia Basin, Offshore Washington State, British Columbia (No. DE-LDEO-FE0029219-1). Columbia Univ, New York, NY (United States) doi:10.2172/1488562.

Goldberg, D.S., Nawaz, S., Lavin, J., Slagle, A.L., 2023. Upscaling DAC hubs with wind energy and CO2 mineral storage: considerations for large-scale carbon removal from the atmosphere. Environ. Sci. Technol. doi:10.1021/acs.est.3c03492.

Gutknecht, V., Snæbjörnsdóttir, S.Ó., Sigfússon, B., Aradóttir, E.S., Charles, L., 2018. Creating a carbon dioxide removal solution by combining rapid mineralization of CO2 with direct air capture. Energy Procedia 146, 129–134. doi:10.1016/j.egypro.2018.07.017.

Hersbach, H., Bell, B., Berrisford, P., Biavati, G., Horányi, A., Muñoz Sabater, J., Nicolas, J., Peubey, C., Radu, R., Rozum, I., Schepers, D., Simmons, A., Soci, C., Dee, D., Thépaut, J.N., 2018. ERA5 hourly data on single levels from 1979 to present.

Hornbostel, K., Lieber, A., Riveroa, J., Hildebrandt, D., Snodgrass, C., Gamble, W., Neal, Z., Davidson, S., Usman, H., Niepa, T.H.R., 2022. Direct ocean carbon capture using membrane contactors. 10.2139/ssrn.4272912

IEA, 2023. CCUS Projects Explorer – Data Tools [WWW Document]. IEA. https://www.iea.org/data-and-statistics/data-tools/ccus-projects-explorer (accessed 8.3.23).
Intergovernmental Panel on Climate Change, 2023. Climate change 2023: synthesis report. Geneva, Switzerland.
Ishaq, H., Crawford, C., 2022. Potential of offshore wind energy for direct air capture. Int. J. Energy Res. 46, 18919–18927. doi:10.1002/er.8506.
Kearns, D.D., 2021. Technology readiness and costs of CCS 50.
Keith, D.W., Holmes, G., St Angelo, D., Heidel, K., 2018. A process for capturing CO2 from the atmosphere. Joule 2, 1573–1594. doi:10.1016/j.joule.2018.05.006.
Kim, S., Nitzsche, M.P., Rufer, S.B., Lake, J.R., Varanasi, K.K., Hatton, T.A., 2023. Asymmetric chloride-mediated electrochemical process for CO2 removal from oceanwater. Energy Environ. Sci. 16, 2030–2044. doi:10.1039/D2EE03804H.
Luo, J., Xie, Y., Hou, M.Z., Xiong, Y., Wu, X., Lüddeke, C.T., Huang, L., 2023. Advances in subsea carbon dioxide utilization and storage. Energy Rev. 2, 100016. doi:10.1016/j.enrev.2023.100016.
Müller, R.D., Zahirovic, S., Williams, S.E., Cannon, J., Seton, M., Bower, D.J., Tetley, M.G., Heine, C., Breton, E.L., Liu, S., Russell, S.H.J., Yang, T., Leonard, J., Gurnis, M., 2019. A global plate model including lithospheric deformation along major rifts and orogens since the triassic. Tectonics 38, 1884–1907. doi:10.1029/2018TC005462.
Madhu, K., Pauliuk, S., Dhathri, S., Creutzig, F., 2021. Understanding environmental trade-offs and resource demand of direct air capture technologies through comparative life-cycle assessment. Nat. Energy 6, 1035–1044. doi:10.1038/s41560-021-00922-6.
Marieni, C., Henstock, T.J., Teagle, D.A.H., 2013. Geological storage of CO2 within the oceanic crust by gravitational trapping. Geophys. Res. Lett. 40, 6219–6224. doi:10.1002/2013GL058220.
IHS Markit (2022) *Energy Cost and Technology Indexes | IHS Markit*. Available at: https://ihsmarkit.com/info/cera/ihsindexes/index.html (accessed 7.13.22).
Matter, J.M., Broecker, W.S., Stute, M., Gislason, S.R., Oelkers, E.H., Stefánsson, A., Wolff-Boenisch, D., Gunnlaugsson, E., Axelsson, G., Björnsson, G., 2009. Permanent carbon dioxide storage into basalt: the CarbFix pilot project, Iceland. Energy Procedia Greenh. Gas Control Technol. 9 1, 3641–3646. doi:10.1016/j.egypro.2009.02.160.
Matter, J.M., Stute, M., Snæbjörnsdottir, S.Ó., Oelkers, E.H., Gislason, S.R., Aradottir, E.S., Sigfusson, B., Gunnarsson, I., Sigurdardottir, H., Gunnlaugsson, E., Axelsson, G., Alfredsson, H.A., Wolff-Boenisch, D., Mesfin, K., Taya, D.F., de la, R., Hall, J., Dideriksen, K., Broecker, W.S., 2016. Rapid carbon mineralization for permanent disposal of anthropogenic carbon dioxide emissions. Science 352, 1312–1314. doi:10.1126/science.aad8132.
McGrail, B.P., Schaef, H.T., Ho, A.M., Chien, Y.J., Dooley, J.J., Davidson, C.L., 2006. Potential for carbon dioxide sequestration in flood basalts. J. Geophys. Res. Solid Earth 111. doi:10.1029/2005JB004169.
Musial, W., Spitsen, P., Duffy, P., Beiter, P., Marquis, M., Hammond, R., Shields, M., 2022. Offshore Wind Market Report: 2022 Edition. U.S. Department of Energy.
NASEM, 2019. Negative Emissions Technologies and Reliable Sequestration: A Research Agenda. National Academies Press, Washington, D.C. doi:10.17226/25259.
National Geospatial-Intelligence Agency, 2019. World Port Index: Twenty Seventh Edition. Springfield, Virginia.
Nawaz, S., Satterfield, T., 2024. Towards just, responsible, and socially viable carbon removal: lessons from offshore DACCS research for early-stage carbon removal projects. Environ. Sci. Policy 151, 103633. doi:10.1016/j.envsci.2023.103633.
Nawaz, S., Peterson St-Laurent, G., Satterfield, T., 2023. Public evaluations of four approaches to ocean-based carbon dioxide removal. Clim. Policy 0, 1–16. doi:10.1080/14693062.2023.2179589.
Nelson, C., Goldberg, D., White, M., Slagle, A., 2022. Optimizing injection strategies for co2 storage and mineralization in basalt through multiphase subsurface reservoir simulations. https://doi.org/10.2139/ssrn.4280798
Northern Lights, 2023. Annual Report 2022. Northern Lights.
Oelkers, E.H., Gislason, S.R., Kelemen, P.B., 2023. Moving subsurface carbon mineral storage forward. Carbon Capt. Sci. Technol. 6, 100098. doi:10.1016/j.ccst.2023.100098.
Pathak, M., Slade, R., Pichs-Madruga, R., Ürge-Vorsatz, D., Shukla, P.R., Skea, J., 2022. Climate Change 2022: Mitigation of Climate Change. Contribution of Working Group III to the Sixth Assessment Report of the Intergovernmental Panel on Climate Change Technical Summary. Cambridge University Press, Cambridge, UK and New York, NY, USA Cambridge University Press doi:10.1017/9781009157926.002.
Patterson, T., Kelso, N.V., 2012. World Coastlines, 1:50 Million (2012). Princeton University Digital Maps and Geospatial Data |.
Pilorgé, H., Kolosz, B., Wu, G.C., Freeman, J., 2021. Global Mapping of CDR Opportunities. CDR Primer.
Planke, S., Bellwald, B., Millett, J., Planke, E.E.E., Zastrozhnov, D., Carlevaris, P., Rosenqvist, M., Jerram, D.A., Schmid, D., Berndt, C., Kjølhamar, B., Myklebust, R., 2021. Permanent carbon sequestration potential in offshore basalt sequences on the NW European Continental Margins. In: Proceedings of the 82nd EAGE Annual Conference & Exhibition. European Association of Geoscientists & Engineers, pp. 1–5. doi:10.3997/2214-4609.202011841.
Pogge von Strandmann, P.A.E., Burton, K.W., Snæbjörnsdóttir, S.O., Sigfússon, B., Aradóttir, E.S., Gunnarsson, I., Alfredsson, H.A., Mesfin, K.G., Oelkers, E.H., Gislason, S.R., 2019. Rapid CO2 mineralisation into calcite at the CarbFix storage site quantified using calcium isotopes. Nat. Commun. 10, 1983. doi:10.1038/s41467-019-10003-8.
Rivero, J., Lieber, A., Snodgrass, C., Neal, Z., Hildebrandt, M., Gamble, W., Hornbostel, K., 2023. Demonstration of direct ocean carbon capture using hollow fiber membrane contactors. Chem. Eng. J. 470, 143868. doi:10.1016/j.cej.2023.143868.
Rosenqvist, M.P., Meakins, M.W.J., Planke, S., Millett, J.M., Kjøll, H.J., Voigt, M.J., Jamtveit, B., 2023. Reservoir properties and reactivity of the Faroe Islands Basalt Group: investigating the potential for CO2 storage in the North Atlantic Igneous Province. Int. J. Greenh. Gas Control 123, 103838. doi:10.1016/j.ijggc.2023.103838.
Rueda, O., Mogollón, J.M., Tukker, A., Scherer, L., 2021. Negative-emissions technology portfolios to meet the 1.5 °C target. Glob. Environ. Chang. 67, 102238. doi:10.1016/j.gloenvcha.2021.102238.
Ryan, W.B.F., Carbotte, S.M., Coplan, J.O., O'Hara, S., Melkonian, A., Arko, R., Weissel, R.A., Ferrini, V., Goodwillie, A., Nitsche, F., Bonczkowski, J., Zemsky, R., 2009. Global multi-resolution topography synthesis. Geochem. Geophys. Geosyst. 10. doi:10.1029/2008GC002332.
Sandalow, D., Aines, R., Friedmann, J., McCormick, C., Sanchez, D., 2021. Biomass carbon removal and storage (BiRCS) ROADMAP (No. LLNL-TR–815200, 1763937, 1024342). https://doi.org/10.2172/1763937
Satterfield, T., Nawaz, S., Peterson St-Laurent, G., 2023. Exploring public acceptability of direct air carbon capture with storage: climate urgency, moral hazards and perceptions of the 'whole versus the parts. Clim. Chang. 176. doi:10.1007/s10584-023-03483-7.
Sendi, M., Bui, M., Mac Dowell, N., Fennell, P., 2022. Geospatial analysis of regional climate impacts to accelerate cost-efficient direct air capture deployment. One Earth 5, 1153–1164. doi:10.1016/j.oneear.2022.09.003.
Shehzad, M.F., Ishaq, H., Crawford, C., 2023. Linear programming model predictive control for offshore wind-direct air capture system using battery storage. In: Proceedings of the European Control Conference (ECC), pp. 1–6. doi:10.23919/ECC57647.2023.10178329.
Sigfússon, B., Arnarson, M.Þ., Snæbjörnsdóttir, S.Ó., Karlsdóttir, M.R., Aradóttir, E.S., Gunnarsson, I., 2018. Reducing emissions of carbon dioxide and hydrogen sulphide at Hellisheidi power plant in 2014-2017 and the role of CarbFix in achieving the 2040 Iceland climate goals. Energy Procedia 146, 135–145. doi:10.1016/j.egypro.2018.07.018.
Slagle, A.L., Goldberg, D.S., 2011. Evaluation of ocean crustal Sites 1256 and 504 for long-term CO2 sequestration. Geophys. Res. Lett. 38. doi:10.1029/2011GL048613.
Snæbjörnsdóttir, S.Ó., Wiese, F., Fridriksson, T., Ármansson, H., Einarsson, G.M., Gislason, S.R., 2014. CO2 storage potential of basaltic rocks in Iceland and the oceanic ridges. Energy Procedia 4585–4600. doi:10.1016/j.egypro.2014.11.491, 12th International Conference on Greenhouse Gas Control Technologies, GHGT-12 63.
Snæbjörnsdóttir, S.Ó., Sigfússon, B., Marieni, C., Goldberg, D., Gislason, S.R., Oelkers, E.H., 2020. Carbon dioxide storage through mineral carbonation. Nat. Rev. Earth Environ. 1, 90–102. doi:10.1038/s43017-019-0011-8.
Sohoni, V., Gupta, S.C., Nema, R.K., 2016. A critical review on wind turbine power curve modelling techniques and their applications in wind based energy systems. J. Energy 2016, e8519785. doi:10.1155/2016/8519785.
Straume, E.O., Gaina, C., Medvedev, S., Hochmuth, K., Gohl, K., Whittaker, J.M., Fattah, R.A., Doornenbal, J.C., Hopper, J.R., 2019. GlobSed: updated total sediment thickness in the world's oceans. Geochem. Geophys. Geosyst. 20, 1756–1772. doi:10.1029/2018GC008115.
Tanaka, Y., Sawada, Y., Tanase, D., Tanaka, J., Shiomi, S., Kasukawa, T., 2017. Tomakomai CCS demonstration project of Japan, CO2 injection in process. Energy Procedia 114, 5836–5846. doi:10.1016/j.egypro.2017.03.1721, 13th International Conference on Greenhouse Gas Control Technologies, GHGT-13, 14-18 November 2016, Lausanne, Switzerland.
Tutolo, B.M., Awolayo, A., Brown, C., 2021. Alkalinity generation constraints on basalt carbonation for carbon dioxide removal at the gigaton-per-year scale. Environ. Sci. Technol. 55, 11906–11915. doi:10.1021/acs.est.1c02733.
Vestas Wind Systems A/S, 2021. Vestas offshore portfolio V236-15.0 MW™.
Webb, C., Vugt, M., 2017. Offshore construction–installing the world's deepest FPSO development. https://doi.org/10.4043/27655-MS
Webster, S.R., Ishaq, H., Crawford, C., 2024. Scaling considerations and optimal control for an offshore wind powered direct air capture system. J. Phys. Energy doi:10.1088/2515-7655/ad31ba.
White, S.K., Spane, F.A., Schaef, H.T., Miller, Q.R.S., White, M.D., Horner, J.A., McGrail, B.P., 2020. Quantification of CO2 mineralization at the Wallula Basalt pilot project. Environ. Sci. Technol. 54, 14609–14616. doi:10.1021/acs.est.0c05142.
Wilcox, J., Kolosz, B., Freeman, J., 2021. CDR Primer.
Xu, Y., Liu, S., Edwards, J.P., Xiao, Y.C., Zhao, Y., Miao, R.K., Fan, M., Chen, Y., Huang, J.E., Sargent, E.H., Sinton, D., 2023. Regeneration of direct air CO2 capture liquid via alternating electrocatalysis. Joule 7, 2107–2117. doi:10.1016/j.joule.2023.07.011.
Young, J., McQueen, N., Charalambous, C., Foteinis, S., Hawrot, O., Ojeda, M., Pilorgé, H., Andresen, J., Psarras, P., Renforth, P., Garcia, S., van der Spek, M., 2023. The cost of direct air capture and storage can be reduced via strategic deployment but is unlikely to fall below stated cost targets. One Earth 6, 899–917. doi:10.1016/j.oneear.2023.06.004.
ZEP, 2011. The costs of CO2 transport: post-demonstration CCS in the EU. European Technology Platform for Zero Emission Fossil Fuel Power Plants, Brussels, Belgium.
ZEP, 2011. The costs of CO2 storage: post-demonstration CCS in the EU.